



HAL
open science

Challenging level of rigid-body approach involving numerical elements (CHLORAINÉ) applied to repeated elastin peptides

C. Depenveiller, H. Wong, J.M. Crowet, Laurent Debelle, S. Baud, Manuel Dauchez, N. Belloy

► To cite this version:

C. Depenveiller, H. Wong, J.M. Crowet, Laurent Debelle, S. Baud, et al.. Challenging level of rigid-body approach involving numerical elements (CHLORAINÉ) applied to repeated elastin peptides. *Journal of Structural Biology*, 2023, 215 (3), pp.107986. 10.1016/j.jsb.2023.107986 . hal-04141914

HAL Id: hal-04141914

<https://hal.univ-reims.fr/hal-04141914v1>

Submitted on 26 Jun 2023

HAL is a multi-disciplinary open access archive for the deposit and dissemination of scientific research documents, whether they are published or not. The documents may come from teaching and research institutions in France or abroad, or from public or private research centers.

L'archive ouverte pluridisciplinaire **HAL**, est destinée au dépôt et à la diffusion de documents scientifiques de niveau recherche, publiés ou non, émanant des établissements d'enseignement et de recherche français ou étrangers, des laboratoires publics ou privés.

Journal of Structural Biology

Challenging Level Of Rigid-body Approach Involving Numerical Elements (CHLORINE) applied to repeated elastin peptides.

--Manuscript Draft--

Manuscript Number:	JSB-23-82R1
Article Type:	VSI: Protein with Tandem Repeats
Keywords:	mesoscopic simulations, multiscale approach, repeated elastin-like peptides, elastomeric polymers, extracellular matrix
Corresponding Author:	Nicolas Belloy Université de Reims Champagne Ardenne Reims, Champagne-Ardenne FRANCE
First Author:	Camille Depenveiller, PhD
Order of Authors:	Camille Depenveiller, PhD Hua Wong, PhD Jean-Marc Crowet, PhD Laurent Debelle, PhD Stéphanie Baud, PhD Manuel Dauchez, PhD Nicolas Belloy, PhD
Abstract:	Elastic proteins and derived biomaterials contain numerous tandemly repeated peptides along their sequences, ranging from a few copies to hundreds. These repetitions are responsible for their biochemical, biological and biomechanical properties. These sequences are considered to be intrinsically disordered, and the variations in their behavior are actually mainly due to their high flexibility and lack of stable secondary structures originating from their unique amino acid sequences. Consequently, the simulation of elastic proteins and large elastomeric biomaterials using classical molecular dynamics is an important challenge. Here, we propose a novel approach that allows the application of the DURABIN protocol to repeated elastin-like peptides (r-ELPs) in a simple way. Four large r-ELPs were studied to evaluate our method, which was developed for simulating extracellular matrix proteins at the mesoscopic scale. After structure clustering applied on molecular dynamic trajectories of constitutive peptides (5-mers and 6-mers), the main conformations were used as starting points to define the corresponding primitives, further used as rigid body fragments in our program. Contributions derived from electrostatic and molecular hydrophobicity potentials were tested to evaluate their influence in the interactions during simple mesoscopic simulations. The CHLORINE approach, despite the thinner granularity due to the size of the patterns used, was included in the DURABIN protocol and emerges as a promising way to simulate elastic macromolecular systems.
Suggested Reviewers:	Sergey Samsonov, PhD Project Leader at Laboratory of Molecular Modeling, University of Gdansk sergey.samsonov@ug.edu.pl specialist of Molecular Modeling in the field of Extracellular Matrix Carlos Rodriguez-Cabello, PhD Pr, University of Valladolid cabello@bioforge.uva.es specialist of Elastin and ELPs Brigida Bocchichio, PhD Pr, University of Basilicata brigida.bochicchio@unibas.it Specialist of Elastin and ELPs

Challenging Level Of Rigid-body Approach Involving Numerical Elements (CHLORINE)

applied to repeated elastin peptides.

C. Depenveiller^{1,3}, H. Wong^{1,2}, J.M. Crowet^{1,2}, L. Debelle¹, S. Baud^{1,2}, M. Dauchez^{1,2}, N. Belloy^{1,2*}

Address

¹ Université de Reims Champagne Ardenne, CNRS, MEDyC UMR 7369, 51097 Reims, France

² Université de Reims Champagne Ardenne, Plateau de Modélisation Moléculaire Multi-Echelle (P3M), Maison de la simulation de Champagne Ardenne (MaSCA), 51097 Reims, France

³ current address: Université de Picardie Jules Verne, CNRS, GEC UMR 7025, 80039 Amiens, France

* corresponding author: nicolas.belloy@univ-reims.fr

Abstract

Elastic proteins and derived biomaterials contain numerous tandemly repeated peptides along their sequences, ranging from a few copies to hundreds. These repetitions are responsible for their biochemical, biological and biomechanical properties. These sequences are considered to be intrinsically disordered, and the variations in their behavior are actually mainly due to their high flexibility and lack of stable secondary structures originating from their unique amino acid sequences. Consequently, the simulation of elastic proteins and large elastomeric biomaterials using classical molecular dynamics is an important challenge. Here, we propose a novel approach that allows the application of the DURABIN protocol to repeated elastin-like peptides (r-ELPs) in a simple way. Four large r-ELPs were studied to evaluate our method, which was developed for simulating extracellular matrix proteins at the mesoscopic scale. After structure clustering applied on molecular dynamic trajectories of constitutive peptides (5-mers and 6-mers), the main conformations were used as starting points to define the corresponding primitives, further used as rigid body fragments in our program. Contributions derived from electrostatic and molecular hydrophobicity potentials were tested to evaluate their influence in the interactions during simple mesoscopic simulations. The CHLORINE approach, despite the thinner granularity due to the size of the patterns used,

32 was included in the DURABIN protocol and emerges as a promising way to simulate elastic
33 macromolecular systems.

34

35 **Keywords**

36 mesoscopic simulations, multiscale approach, repeated elastin-like peptides, elastomeric
37 polymers, extracellular matrix

38

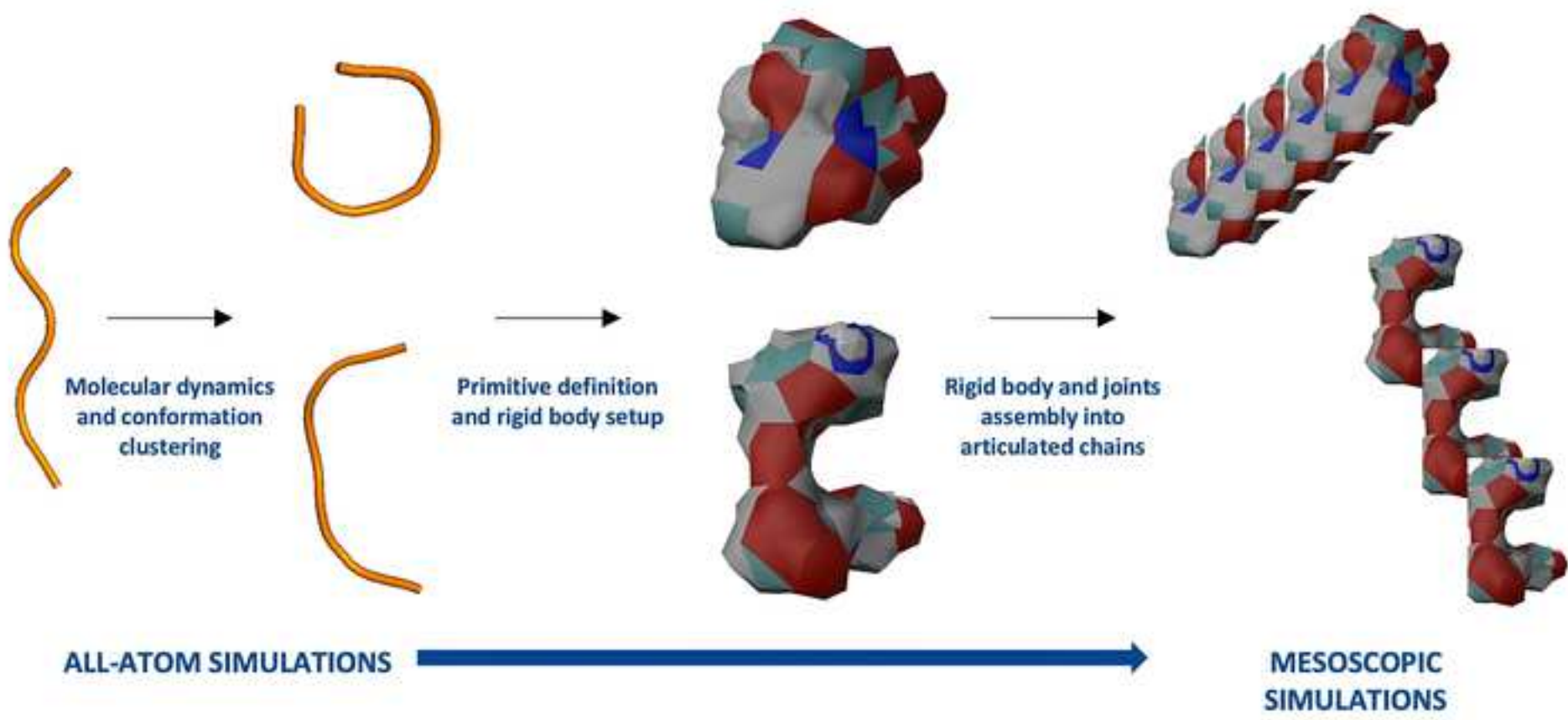
39 **Abbreviations**

40 ECM, extracellular matrix; r-ELPs, repeated elastin-like peptides

41

1
2
3
4
5
6
7
8
9
10
11
12
13
14
15
16
17
18
19
20
21
22
23
24
25
26
27
28
29
30
31
32
33
34
35
36
37
38
39
40
41
42
43
44
45
46
47
48
49
50
51
52
53
54
55
56
57
58
59
60
61
62
63
64
65

1
2
3
4
5
6
7
8
9
10
11
12
13
14
15
16
17
18
19
20
21
22
23
24
25
26
27
28
29
30
31
32
33
34
35
36
37
38
39
40
41
42
43
44
45
46
47
48
49



- Elastin, its monomer tropoelastin and repeated elastin-like peptides (r-ELPs) are of great interest in the field of biomaterials and biocompatibility.
- Classical molecular dynamics methods are not always suitable for the simulation of long sequences with tandem repeats.
- Rigid body dynamics allows the simulation of very large molecular systems of the extracellular matrix.
- This new way to simulate r-ELPs helps in the study of very large macrosystems and/or biomaterials with repeated patterns.

1
2
3
4
5
6
7
8
9
10
11
12
13
14
15
16
17
18
19
20
21
22
23
24
25
26
27
28
29
30
31
32
33
34
35
36
37
38
39
40
41
42
43
44
45
46
47
48
49
50
51
52
53
54
55
56
57
58
59
60
61
62
63
64
65

42 Introduction

1
2 43 Elastomeric proteins are found throughout biology in numerous different species
3
4 44 (Muiznieks and Keeley, 2017). They demonstrate a large amount of mechanical properties
5
6 45 that allow characteristic mechanisms such as extensibility, stiffness, tensile strength and many
7
8 46 other properties. Most of these elastic proteins present tandemly repeated sequences and, at
9
10 47 the supramolecular level, they may also propose series of tandemly-repeated proteins (Jorda
11
12 48 et al., 2010). The repeated motifs of these elastomers arise from specific sequences. In the
13
14 49 case of abductin, a protein from bivalve mollusks, two consensus sequences are found,
15
16 50 GGFGGMGGG and GFFMGGGNAG (Cao et al., 1997). In insects, resilin harbors the following
17
18 51 repeated motifs, GGRPSDSYGAPGGGN, AQTSSQYPAG (Lyons et al., 2007). In spider silk
19
20 52 fibroins, the fragments GAGAGS and GAGAGY are present in numerous motifs (Zhou, 2000).
21
22 53 In mammals, titin, collagens and elastin (Gosline et al., 2002), proteins found in vertebrate
23
24 54 muscles and connective tissues respectively, present a significant number of tandemly
25
26 55 repeated patterns.

27 56 We have focused our work for several decades on the study and role of elastin in the
28
29 57 extracellular matrix (ECM). Elastin is an essential component of various tissues that require
30
31 58 elasticity. In humans, elastin endows the ability to stretch and recoil to skin, lungs and large
32
33 59 arteries, thereby playing an important role in their physiological function (Le Page et al., 2019).

34
35 60 Tropoelastin, the constitutive monomer of the elastin, is a very peculiar structural protein
36
37 61 and unfortunately the structure of this protein remains unknown, since X-rays crystallography
38
39 62 and/or Nuclear Magnetic Resonance methods failed to unravel this structure at the atomic
40
41 63 level. Tarakanova et al. have proposed a 698 residue-long tropoelastin model using SAXS
42
43 64 experimental methods in conjunction with molecular modeling simulations (Tarakanova et al.,
44
45 65 2018). However, the use of this model is limited, since the data is an envelope (no atomic
46
47 66 coordinates) and this envelope only accounts for a single conformation, which is reductive
48
49 67 compared to the inherent flexibility of tropoelastin.

50 68 Several studies using molecular dynamics with both all-atom and/or coarse-grained force
51
52 69 fields have been published on constitutive peptides of tropoelastin (Seo et al., 2012). Although
53
54 70 these simulations lead to comprehensive behaviors of elastin-like peptides (ELPs), their
55
56 71 structure-function dynamics relationships are still not easily obtained, be it for elastic peptides
57
58 72 or larger molecular systems. Most all-atom simulations are performed using force fields
59
60 73 derived from amino acid peptides found in globular proteins. CHARMM36m (Huang et al.,
61
62
63
64
65

74 2017) has been developed to better understand (among other systems) intrinsically
75 disordered proteins. However, it is not really suitable for simulations of elastomeric proteins
76 and/or elastic properties, which remain a challenging task.

77 As discussed above, the very nature of tropoelastin sequence contributes to the
78 limitations of this type of simulation. Full-length human tropoelastin comprises 786 residues
79 and 82% of its sequence consists of only 5 amino acids: glycine (221), alanine (164), valine
80 (98), proline (96), leucine (45), found in numerous repetitive and overlapping patterns. Among
81 these, some 5-mers and 6-mers are found several times.

82 Due to the lack of dedicated numerical methods, numerical simulations of large elastic
83 peptides or biomaterials are extremely difficult, if not impossible with current methods. Since
84 2014, we develop a very efficient mesoscopic rigid body approach to simulate very large multi-
85 domains in the ECM (Wong et al., 2018). We have used the Unity3D game and physics engines
86 (along with rigid body dynamics) to propose an application called DURABIN. Using this
87 method, it is possible to study tens to hundreds of proteins in a very simple way. We have
88 validated our approach by studying a peculiar ECM environment, the basement membrane.

89 In this work, we propose a proof of concept using our mesoscopic tool DURABIN to study
90 elastic systems derived from tandem r-ELPs. This work leads to the Challenging Level Of Rigid-
91 body Approach Involving Numerical Elements - CHLORAINE method applied to r-ELPs. In a
92 multi-scale understanding of biological systems, our study attempts to better decipher the
93 structure/dynamics of homopolymers of small peptides. Indeed, insight into the mesoscopic
94 details of biopolymers derived from elastin is particularly important for understanding the
95 molecular mechanisms underlying their functions.

96 1. Methods & Materials

97 1.1 Peptides

98 Elastin and its constitutive monomer tropoelastin possess numerous repeated
99 fragments that allow the function of these molecules. In this work, the corresponding selected
100 motifs arise from r-ELP penta-peptides VPGXG with X as V, E or K amino acids and hexa-
101 peptides VGZAPG with Z as V or L amino acids. The 4 following homopolymers were
102 investigated:

103 poly-VPGVG: (VPGVG)₂₇

104 poly-VPGEG: (VPGEG)₂₇

106 poly-VPGKG: (VPGKG)₂₇
107 poly-exon24-like: [(VGLAPG)(VGVAPG)₂]₂₇
108 leading to a respective length of 135 amino acids for the three first peptides, and of 486 amino
109 acids for the last one. n=27 has been identified as a “minimal” length of homopolymers used
110 in biomaterial experimental works for the first 3 sequences (Rodriguez-Cabello et al., 2021),
111 and the last sequence is correlated with the motif found in the exon 24 of human-TE and used
112 as mini-elastin fragment by F. Keeley (Muiznieks and Keeley, 2017). For the (VPGXG)₂₇
113 polypeptides, the role of the X amino acid is evaluated. The comparison with the poly-exon24-
114 like homopolymer allows to study the impact of the primitive length (a building block of 5
115 amino acids for (VPGXG)₂₇ compared to a building block of 18 amino acids for
116 [(VGLAPG)(VGVAPG)₂]₂₇).

117

118 1.2 Molecular dynamics simulations

119 Similar modeling and molecular dynamics simulation procedures were used for each
120 individual repeat peptide (5-mers or 6-mers). Each r-ELP was built in an extended
121 conformation using PyMOL (The PyMOL Molecular Graphics System, Version 2.0 Schrödinger,
122 LLC). After 50,000-step minimization using a steepest descent algorithm, 100-ps NVT
123 equilibration and 100-ps NPT equilibration, multiple 500-ns molecular dynamics simulations
124 were performed using GROMACS software (Berendsen et al., 1995) with the OPLS-AA/L force
125 field. Each peptide was solvated in a cubic water box with a generic equilibrated 3-point
126 solvent model (TIP3P), and with a distance of 1 nm between the solute and the box. Na⁺ and
127 Cl⁻ ions were added at a concentration of 0.15 M.

128 After running the production step of molecular dynamics, the conformations of the
129 peptides along the trajectories were visualized with VMD (Humphrey et al., 1996).

130

131 1.3 Clustering leading to the design of primitives

132 To obtain the major conformations for each of these peptides, we have performed
133 clustering on the conformations sampled during the trajectory, allowing us to distribute the
134 different conformations in different groups. The clustering tool *gmx cluster* with GROMOS
135 method (Daura et al., 1999) available in GROMACS and the TTClust algorithm (Tubiana et al.,
136 2018) have been used to access the major conformations. In the latter method, a distance
137 matrix containing the RMSD values between all pairs of frames of the trajectory is generated.

1
2
3
4
5
6
7
8
9
10
11
12
13
14
15
16
17
18
19
20
21
22
23
24
25
26
27
28
29
30
31
32
33
34
35
36
37
38
39
40
41
42
43
44
45
46
47
48
49
50
51
52
53
54
55
56
57
58
59
60
61
62
63
64
65

138 A second matrix is then generated from this distance matrix using a hierarchical clustering
139 function, so that a dendrogram of this matrix can be generated. For each motif observed in
140 our r-ELPs, this clustering allowed us to identify the main clusters.

141 The Blender software (<https://www.blender.org>) is then used to generate
142 representations of the main conformations derived from the clustering step. These
143 representations, called primitives, are simplified shapes describing the conformations of the
144 peptide. The primitives are used as “blocks” to represent r-ELP motifs in the DURABIN
145 mesoscope.

146

147 *1.4 Electrostatic and molecular hydrophobicity potentials*

148 In order to evaluate the influence of physicochemical properties of our different elastic
149 peptides, we have performed the Adaptive Poisson-Boltzmann Solver (APBS) to determine
150 electrostatic contributions. APBS is a method for the numerical solution of the Poisson-
151 Boltzmann equation, a continuum model for describing electrostatic interactions (Holst and
152 Saied, 1995). Knowledge of the electrostatic positive and negative contributions is very
153 important to understand the interactions between different molecules. In the case of r-ELPs,
154 due to their intrinsic functional flexibility, these contributions are observed on the whole
155 peptide, but are also present along the chain, around peptide bonds.

156 In the same way, we used molecular hydrophobicity potential (MHP) (Brasseur, 1991)
157 to get hydrophobic and hydrophilic contributions. The calculation of the MHP along r-ELPS is
158 based on the molecular lipophilicity potential (Furet et al., 1988) and the hydrophobicity
159 potential developed by Fauchère (Fauchère et al., 1988). These parameters are defined by
160 considering a molecule surrounded by organic solvent molecules and by assuming that the
161 overall hydrophobicity is the sum of the hydrophobicity of its different atoms as described by
162 Lins et al. (Lins et al., 2003).

163 By using the electrostatics and hydrophobicity/hydrophilicity potentials computed as
164 explained above, we could obtain and display, on the peptide surface, the corresponding
165 surfaces of positive/negative electrostatics and hydrophobicity/hydrophilicity. From our
166 simulations of tropoelastin peptides, it appears that electrostatics correspond to smaller
167 surfaces, thus weaker contributions, compared to hydrophilicity/hydrophobicity ones and the
168 hydrophobic areas are much more important than the hydrophilic areas even if this latter

169 cannot be neglected. Knowing the size of each area is very important to define correctly the
170 corresponding shapes in the DURABIN mesoscope.

171

172 *1.5 Rigid body simulations*

173 Once the primitives have been created with Blender and validated, they are used in
174 Unity3D (<https://unity.com>) to apply the rigid body approach. Unity3D is a cross-platform
175 game engine that has many applications beyond video games, such as data visualization of
176 simulation trajectories. Some software packages are chosen for modeling and simulations in
177 the virtual reality model DURABIN and are therefore also used to apply the rigid body
178 approach to the case of tropoelastin at the mesoscopic scale. In Unity3D, we use the primitives
179 set up from Blender to define rigid bodies and model polypeptides as it was previously done
180 for protein domains (Wong et al., 2022). Indeed, the first step is to set up colliders on the
181 primitives. Colliders are components that define the shape and occupancy of objects in space.
182 For a given primitive, the number and spatial arrangement of colliders depends entirely on
183 the conformation of the relative primitive, as well as on the presence (or not) of
184 hydrophilicity/hydrophobicity and/or electrostatic contributions. This step allows to set up
185 the rigid body corresponding to the primitive/conformation under consideration. This process
186 is repeated for each conformation we want to take into account, in order to build a library of
187 rigid bodies representing the different motifs of tropoelastin.

188 In this protocol applied to elastin polypeptides, the difference with the original
189 DURABIN is the granularity in the representation of the molecules. Indeed, in DURABIN the
190 proteins are modeled by rigid bodies corresponding to domains of 100-200 amino acids.
191 However, in the CHLORAINE method, the granularity is thinner but still larger than for coarse-
192 grained simulations which use designed beads of a few atoms. The CHLORAINE approach
193 defines rigid bodies in elastin polypeptides corresponding rather to tropoelastin motifs of 5 to
194 18 amino acids.

195 The next step is to use the rigid bodies also called building blocks from the library, in
196 order to model longer polypeptides with motifs from tropoelastin. A polypeptide can be made
197 up of several rigid bodies (of the same type or of different types) connected by molecular
198 joints. These joints are objects that represent physical constraints and that we specifically
199 define in this work so that they act as articulations between rigid bodies. Indeed, joints are set

200 up to describe angular constraints through Phi and Psi angles that can be adapted to each
201 motif.

202 Once the polypeptides are modeled, they can be simulated and the DURABIN simulator
203 allows to compute contacts between rigid bodies during the simulation. In this way, we can
204 get this data and provide matrices of intramolecular (between rigid bodies from the same
205 polypeptide) and intermolecular (between rigid bodies from different polypeptides)
206 interactions.

207 Thereby, elastomeric polypeptides can be modeled as articulated chains of small rigid
208 bodies and simulated at the mesoscopic scale.

209 210 **2. Results – Discussion**

211 Simulation of very large molecular systems remains a very complicated task, despite
212 recent progress such as coarse-grained force fields and the optimization of molecular
213 dynamics software running on Graphical Process Unit GPU. Very recently, we have developed
214 a very simple method, called DURABIN, to study the crowding of proteins (Wong et al., 2018).
215 This method uses the rigid body approach to study the ECM in a mesoscopic environment. In
216 the simulated model, each rigid body, also called a module or a building block, corresponds to
217 a specific structural domain of a protein. The proteins already present in the model are type
218 IV collagen, laminin, nidogen, integrins, and perlecan (Wong et al., 2022). For these proteins,
219 the rigid bodies, defined to fully model them, correspond to each constitutive domain/module
220 of the protein studied. So far, in DURABIN, rigid bodies represent domains ranging from 50 to
221 200-300 amino acids and a primitive volume is used to represent the corresponding domain.
222 The organization of the basement membrane is well known. Further, structures of its
223 constitutive proteins are available. It is therefore simple to obtain simulations with 100
224 different proteins using this approach. Structural data for elastin and tropoelastin are very
225 scarce. Weiss and co-workers (Tarakanova et al., 2018) have proposed some models and
226 simulations using data from SAXS experiments. Using the SAXS envelope, we have compared
227 the sizes of basement membrane type IV collagen (Fig. 1A) and tropoelastin (Fig. 1B) and the
228 corresponding association of 4 tropoelastin monomers as proposed by Weiss and co-authors
229 (Fig. 1C).

230 Up to now, the DURABIN methodology is very efficient to simulate large systems with
231 important domains. To be able to model and simulate more complete and complex ECM

232 elements with this approach, it is imperative to implement additional ECM macromolecules
233 in DURABIN catalogue/database. In this respect, the application of *in silico* approaches for a
234 granularity corresponding to molecules characterized by repetitive motifs can be particularly
235 promising.

236 As a proof of concept, we have chosen to consider some of the individual characteristic
237 patterns of tropoelastin, which are often used as building blocks in biomaterials. To simplify
238 the discussion, in the text below (VPGVG)₂₇ will be referred as VPGVG, (VPGEV)₂₇ and
239 (VPGKG)₂₇ as VPGEV and VPGKG respectively, and [VGLAPG(VGVAPG)₂]₂₇ as Exon24, as it is
240 derived from human tropoelastin exon 24-encoded sequence. In the CHLORAINE approach,
241 one primitive corresponds to 5 or 6 amino acids (namely 5-mer and 6-mer) for single motif,
242 up to 15 and 18 amino acids for di- and tri-motifs. The granularity is thinner than in the initial
243 DURABIN where rigid bodies correspond to whole protein domains. Therefore, considering
244 DURABIN and CHLORAINE method, rigid bodies introduced into the model are either protein
245 domains or peptides of different lengths. However, even if the granularity is different, the
246 process of defining the primitives and the corresponding rigid bodies, and the scaling up to
247 the mesoscopic scale is the same for the domains and the motifs, making this method a
248 multiscale approach.

2.1 Molecular dynamics of peptides and acquisition of future primitives

251 In a first step, we have performed molecular dynamics simulations of 1500 ns (3 x 500
252 ns trajectories) for each building block (VPGVG, VPGEV, VPGKG and VGLAPG(VGVAPG)₂). From
253 the trajectories, we have performed clustering, using the GROMOS and TTClust methods, to
254 obtain characteristic conformations of each block. Since the number of clusters determined
255 at the end of the all-atom simulations is quite large, it is not possible to make an exhaustive
256 library of conformations. Thus, to constitute our library of blocks, we only consider the major
257 conformations, i.e., the conformations that are representative of the main clusters,
258 corresponding to 2 or 3 conformations at most per motif. In Figure 2, we show the major
259 conformations obtained for Exon24 and used as primitives.

260 A primitive is thus derived from a conformation substantially adopted by the peptide,
261 and corresponds to a simplified description of that conformation. A primitive comprises the
262 simplified molecular surface of the considered conformation, as well as additional
263 physicochemical envelopes. These envelopes correspond to the representation of the

264 hydrophobic/hydrophilic and electrostatic properties of the motif. The primitive will influence
1
2 265 the arrangement of the colliders, components that define the shape and the occupancy of the
3
4 266 objects in space, which will define the shape of the rigid body and best match to its shape
5
6 267 (Figure 3). Colliders make it possible to comply the principle of non-overlapping when
7
8 268 assembling several rigid bodies.

9
10 269 Then, each primitive (molecular surface + physicochemical envelopes) with its
11
12 270 colliders, produced with the CHLORAINE method, can be implemented and used in DURABIN.
13
14 271 A library of 38 different building blocks from the different sequences has been proposed and
15
16 272 is used to build some selected homopolymers. In this proof of concept, we only use one
17
18 273 conformation of a motif to build a homopolymer. However, given the flexibility of elastin and
19
20 274 r-ELPs, it will be of great importance to consider several conformations in a polypeptide in our
21
22 275 future works.

23 276

25 277 *2.2 Rigid bodies assembly to build polypeptides at the mesoscopic scale*

26
27 278 By articulating several basic primitives together, polymer assemblies can be created.
28
29 279 Joints are placed between two modules, to link them and articulate the chain in keeping with
30
31 280 the local physical constraints (Figure 3). Two types of joints have been implemented. To
32
33 281 perform a simulation without any angular constraint at the level of a spherical joint, Freely-
34
35 282 Jointed Chains (FJC) joint can be defined as it allows totally free rotations around the bond.
36
37 283 Alternatively, it is possible to use a combination of configurable joints and to define angular
38
39 284 constraints (Phi/Psi), determined from all-atom simulations. These joints are more suitable to
40
41 285 reproduce the degrees of freedom of the local peptide bond, and allow the implementation
42
43 286 of structural constraints derived from all-atom molecular dynamics simulations.

44 287

46 288 *2.3 Modeling and simulations of homopolymers*

47
48 289 The choice of homopolymers to be constructed and simulated was based on four
49
50 290 characteristic peptide motifs representative of tropoelastin.

51
52 291 First, we chose the VGLAPG-(VGVAPG)₂ motif, found in the sequence encoded by exon
53
54 292 24 of the human elastin gene. By tandemly repeating this motif, we created a repeating
55
56 293 (VGVAPG)₂-VGLAPG-(VGVAPG)₂ fragment, which mimics the sequence present in domain 24
57
58 294 of tropoelastin.

59
60
61
62
63
64
65

295 The three other polymers are inspired by polypeptides derived from bovine
1 296 tropoelastin sequence that have been widely used in biomaterials. They all correspond to
2 397 poly-VPGXG sequences, that define classical ELPs. The most common is poly-VPGVG.
3 498

5 298 The constructed homopolymers are: a polymer mimicking human exon 24 encoded
6 299 sequence [VGLAPG-(VGVAPG)₂]₂₇ (this material can be defined as a mini-elastin), a poly-
7 300 VPGVG, (VPGVG)₂₇, a poly-VPGEg, (VPGEg)₂₇, and a poly-VPGKG, (VPGKG)₂₇. The choice of
8 301 building homopolymers consisting of 27 repeats of 5 or 6 residues, say polymers of sizes
9 302 varying between 135 and 486 amino acids, matches the minimal sizes of ELPs designed for
10 303 biomedical approaches (MacEwan and Chilkoti, 2014)(Rodríguez-Cabello et al.,
11 304 2016)(Rodríguez-Cabello et al., 2021).
12 13 14 15 16 17 18

19 305 For each type of polypeptide, simulations were first carried out on polypeptides where
20 306 primitives were based on the molecular surface of the corresponding peptide unit. Further,
21 307 mesoscopic simulations were performed to assess their behavior in terms of
22 308 hydrophilic/hydrophobic and/or electrostatic interactions. These simulations were performed
23 309 by adding, in the definition of the primitives, firstly, the hydrophilic/hydrophobic surfaces,
24 310 then the positively/negatively charged surfaces, and, finally, all properties. In Figure 4, a copy
25 311 of each homopolymer used in the simulations is given in an extended initial conformation.
26 312 Then, as a proof of concept, we ran simulations with 10 copies of the considered polypeptide,
27 313 to be able to study, in addition to the intramolecular interactions, the intermolecular
28 314 interactions that exist between motifs of different polypeptides. For each type of simulation,
29 315 the size of the box had to be adapted. Consequently, the box used for the (VPGXG)₂₇
30 316 simulations could not be kept for [VGLAPG-(VGVAPG)₂]₂₇ simulations, since the size of the
31 317 molecule is 486 instead of 135 amino acids. The box for [VGLAPG-(VGVAPG)₂]₂₇ was therefore
32 318 enlarged to maintain stable simulations.
33 319

320 *2.4 Polypeptide behavior and interactions*

321 Table 1 presents the number of steps reached after running the simulation for a fixed
322 duration, i.e. 60 h, as a function of the biopolymer and added contributions.
323

324 Whatever the considered contribution, the number of steps reached by VPGXG
325 systems are different, although they are very close in terms of size and amino acid contents.
326 This can be explained by the fact that each type of VPGXG have different number of colliders
defined for their rigid bodies. Indeed, a single VPGEg has 2 colliders, whereas a single VPGVG

327 has 3, and a single VPGKG has 4. This means that the VPGEG system (constituted by 27 rigid
1 328 bodies) has 54 colliders, the VPGVG system has 81 colliders, and the VPGKG one has 108
2 329 colliders. In Table 1, the system that reaches the highest number of steps is VPGEG (which has
3 330 the lowest number of colliders), then VPGVG and finally VPGKG (which has the highest number
4 331 of colliders). More colliders implies more computational time for resolving contacts and
5 332 interactions during the simulation. Actually, the number of colliders defined on the peptide
6 333 surface is based on a geometrical aspect and is adapted depending on the
7 334 shape/conformation of the peptide as mentioned above. A single "Exon24" has also 2 colliders
8 335 (Figure 3) but reaches a much lower number of steps than VPGEG. However, it is important to
9 336 note that one rigid body from the VPGXG systems contains 6 amino acids, whereas one rigid
10 337 body from the Exon24 system contains 18 amino acids. Thus, the surface of potential contacts
11 338 is larger for the Exon24 system than for VPGXG systems, resulting in more calculation and a
12 339 lower number of steps reached. Moreover, for a same system, comparing the number of steps
13 340 as a function of contributions (Table 1), we observe that they are very different. The highest
14 341 figures correspond to the neutral condition (no contribution added). With no contribution,
15 342 computing the interactions consists only in counting the number of contacts between the rigid
16 343 bodies. The use of additional contributions implies other calculations, which limits the number
17 344 of steps reached at a given time. In the same way, the simulation of the system with the 2
18 345 contributions reaches the lowest number of steps, except for the VPGKG case.

346 To get insights into this observation, we computed the mean number of intermolecular
347 contacts per simulation step (Table 2).

348 We observed that the number of contacts per step is generally higher with the
349 combination of the two contributions than for the neutral condition (VPGEG: 0.44 for neutral,
350 0.9 for 2 contributions; VPGVG: 0.63 for neutral, 2.36 for 2 contributions). This explains the
351 higher contact computation time and, thus, the lower number of steps reached in the
352 simulation. However, the situation is different for VPGKG. This system must be considered
353 differently since the initial conformation used (the main one obtained from molecular
354 dynamics simulations) is highly folded. That way, a more rigid and smaller model constitutes
355 the rigid body seed. Thus, in this situation, the results concerning contacts computing might
356 be biased.

357 Figure 4 presents the 4 r-ELPs in their elongated forms at the initial step in the
358 simulations. In this figure, the size of the systems can be appreciated and the VPGKG peptide

359 is shorter. This is because the conformation issued from the molecular dynamics clustering of
360 VPGKG is importantly folded as compared to VPGVG and VPGEG. This prevents the rotations
361 around the joints between the rigid bodies from mimicking the real dynamics. The contacts
362 are distorted as they do not reflect the expected interactions. As a result, our method of
363 representing conformations is less suitable for highly folded peptides with close extremities.
364 In this case, we will have to check several other principal conformations arising from the
365 clustering and rather choose a conformation which will lead to more stable simulations at the
366 mesoscopic scale. In other words, we need a conformation respecting the non-superposition
367 principle when building the articulated chain of rigid bodies.

368 Furthermore, for all systems that present only one additional contribution, the number
369 of steps is really different if we consider the hydrophobic/hydrophilic contribution or the
370 electrostatics one. For hydrophobicity (Table 2), the number of contacts per step is higher
371 than for electrostatics (VPGEG: 0.74 for hydrophobicity, 0.32 for electrostatics; VPGVG: 1.03
372 for hydrophobicity, 0.38 for electrostatics). This point explains the higher computation time
373 resulting in the inferior number of steps reached when hydrophobic interactions are
374 considered.

375 The greater importance of hydrophobic/hydrophilic contacts compared to
376 electrostatics ones can be justified by the fact that, in a general way, hydrophobic/hydrophilic
377 surfaces are much larger than electrostatics ones. Thus hydrophobic/hydrophilic interactions
378 are more likely to occur compared to electrostatics ones. We can also notice that the number
379 of steps reached during the neutral simulation is higher than the one reached by the
380 electrostatic simulation, even if the number of neutral contacts is higher than the number of
381 electrostatic contacts. This is because, as said above, the computing time required is more
382 important for the electrostatic contacts compared to the neutral one. To summarize, if we
383 consider one or two contributions, the contact computation time is longer, and thus the
384 simulation reaches less steps. Moreover, simulations with hydrophobicity perform less steps
385 than with electrostatics because there are more hydrophobic interactions occurring than
386 electrostatics ones. Our experiments show that the simulation progression is totally
387 dependent on the choice of the used contributions.

388 In order to assess the performance of the CHLORAINE procedure presented in this
389 work, we have simulated an arbitrary number of 10 chains of each polymer. As discussed
390 above, the size of the box had to be adjusted to maintain stable simulations. The longer the

391 homopolymers simulated, the highest the concentration of molecules in the box for a fixed
392 number of copies. Nevertheless, even in this case, simulations provide nice information about
393 the interaction of the copies and the “local crowding” that may be obtained. In Figure 5, the
394 evolution of 10 chains of [(VGLAPG)(VGVAPG)₂]₂₇ during the first 6,000 steps of a CHLORINE
395 procedure using both electrostatic and MHP potentials is presented. In the initial step, the 10
396 chains are in an extended state in a random position. After few steps of simulation, we
397 observed for all the simulations that the copies bend and interact in a dynamic way. Along the
398 simulations, the different rigid bodies of a copy may interact both in an intramolecular and
399 intermolecular ways. From these simulations, it is possible to derive matrices of interactions
400 and to follow the interactions of the simulated systems. In Figure 6, the matrices of
401 interactions of the polypeptide (VPGEG)₂₇ after 38,000 steps (A) and 128,000 steps (B) of
402 simulation are provided. In this figure, each square (27x27) corresponds to one copy of the
403 polymer (of 27 rigid bodies) and thus each axis represents the 10 copies of (VPGEG)₂₇ put in
404 the simulation box. An interaction matrix is obtained at each step, with the cumulative
405 number of interactions that occurred since the initial step. Thus, it is possible to follow the
406 evolution of the interactions along the simulation. This allows to distinguish how the
407 simulation has progressed during a period of time and which building blocks of the copies
408 have been involved in the interactions. Here, we chose to represent the matrices of
409 intermolecular interactions at 38,000 steps (6A) and 128,000 steps (6B) of simulation. In the
410 same way, in Figure 7, the matrices of interactions at the same step of (VPGVG)₂₇ are provided
411 with dihedral contribution (7A), plus electrostatic contribution (7B), plus
412 hydrophobic/hydrophilic contribution (7C) and all the contributions (7D). Due to the number
413 of colliders used in the simulations, we observe that when the electrostatic contribution is
414 added, we drastically reduce the number of interactions. This is not the case with
415 hydrophobic/hydrophilic parts. When performing the MHP calculations for the isolated
416 peptide, we know that the computed MHP surfaces are much larger than the electrostatic
417 ones. The corresponding primitives defined have thus larger surfaces and, as a consequence,
418 the hydrophilic/hydrophobic contributions are more important in the calculations as seen in
419 Figure 7D, where all the contributions are added.

420 Thanks to the DURABIN mesoscope, it is possible to confidently simulate elastic
421 repeated peptides associated into a “small” (compared to experiments) homopolypeptide.
422 The CHLORINE procedure allows us to modulate the size of the studied rigid bodies and even

423 if the granularity is different, the process of primitives definition and the corresponding rigid
1 424 bodies. The scaling up to the mesoscopic scale is however the same for domains and motifs,
2
3 425 which makes CHLORINE a multiscale approach.
4

5 426 In the near future, we will focus on controlling the size of the simulation boxes, as this
6
7 427 parameter impacts the concentration of r-ELPs. This point is essential to provide reliable
8
9 428 mesoscopic simulations that could then be directly compared to experimental data obtained
10
11 429 for comparable biomaterials.
12

13 430

15 431 **Conclusions - Perspectives**

17 432 In this work, we provide a proof of concept that allows the numerical simulation of r-ELPs
18
19 433 in a simple way. r-ELPs are very important for the design of new elastomeric biomaterials
20
21 434 (Ibáñez-Fonseca et al., 2019). Up to now, the simulation of elastic peptides associated to
22
23 435 biomaterials remains very challenging due to the specificity of r-ELPs sequences, lengths
24
25 436 and/or properties. Very recently, some attempts have been made to compute them in all-
26
27 437 atom or coarse-grained systems (Li et al., 2021)(Baul et al., 2020) but these simulations remain
28
29 438 limited due to the size of the molecular systems. We have adapted our mesoscopic rigid body
30
31 439 modeling system (DURABIN (Wong et al., 2018)) to study molecular objects ranging from very
32
33 440 large multi-domain proteins of the ECM to potential biomaterials made of tandemly repeated
34
35 441 peptides. Here, our Challenging Level Of Rigid-body Approach Involving Numerical Elements
36
37 442 (CHLORINE) method is applied to some chosen r-ELP patterns to evaluate their dynamical
38
39 443 behavior, the associated interactions and the influence of the complexity of the simulations.

40 444 At the same time, it must be emphasized that the high level of the heterogeneity and
41
42 445 complexity of biomaterial simulations represent a possible obstacle to drawing more detailed
43
44 446 and particularly quantitative conclusions. The multiscale approach has been implemented
45
46 447 with the passage from some conformations of small fragments or peptide motifs of
47
48 448 tropoelastin to polypeptides (corresponding to chains of assembled fragments); in other
49
50 449 words, from nanoscale to mesoscale levels. Simplified surfaces called primitives were defined
51
52 450 from those conformations. These primitives determine the setting up of the colliders, which
53
54 451 define the occupancy of the motifs in the space. In this way, the shape of the rigid body
55
56 452 corresponding to each represented conformation is established. Besides,
57
58 453 hydrophilic/hydrophobic and positive/negative electrostatic contributions can be considered
59
60 454 in primitives by adding their corresponding surfaces on the molecular surface of a
61
62
63
64
65

455 conformation. We can thus get the hydrophilic/hydrophobic and electrostatic behavior of r-
456 ELPs, in particular through the study of intra- and interchain interactions.

457 In this paper, we consider homopolymers of main conformations of four tropoelastin
458 units, but it would be interesting to integrate primitives of other conformations for the same
459 motifs. We have tested our approach on three homopolymers (138 AA in length) composed
460 of pentameric peptides (same motif VPGXG with X as V, E or K) and one homopolymer with 6-
461 mer patterns (486 AA in length). The flexible and fractal nature of tropoelastin implies a high
462 number of conformations for a given sequence motif (conformational entropy). Thus, it would
463 be very interesting to perform simulations of heteropolymers, which would be constructed by
464 assembling different motifs (sequences) and/or different conformations: the consequence
465 would be a dramatical increase of the combinatorics. On top of that, we have seen in this
466 paper the issue of highly folded conformations, which need to be treated differently from the
467 others. Indeed, we should improve the way to model these conformations (for instance
468 defined by a certain threshold of radius of gyration), to avoid potentially biased interactions
469 during the simulation.

470 Furthermore, in the near future, mesoscopic simulations will have to take into account the
471 sampling problem and therefore the volume of the simulation boxes. In fact, the size of the
472 simulation box should be adaptable according to the length of the polypeptide studied, thus
473 adapting the concentration of polypeptides. It will therefore be important to optimize this
474 parameter for future simulations and to be able to control the volume, concentration or
475 temperature. Indeed, in DURABIN, it is possible to change the temperature to increase
476 thermal agitation thereby modulating the frictions between macromolecules.

477 Concerning the simulation progression, it will be interesting to study the optimization of
478 the interactions computing. Indeed, by reducing the necessary computational time, our
479 simulation will be able to achieve a more significant number of steps for a given time. It will
480 be necessary to have a calibration between the timestep used in DURABIN and a time
481 duration. Moreover, we have seen that the number of colliders describing the primitive has
482 an influence on computation time. Thus, it is necessary to find a compromise between the
483 number of colliders and the precision of the surface description.

484
485 As a conclusion, the CHLORAINE approach allows to apply the rigid body approach to
486 elastin polypeptides and to integrate them in our simulator, DURABIN (Wong et al., 2018).

487 Thus, we perform simulations of large polypeptides derived from elastin at the mesoscopic
1 488 scale. This achievement is an essential step towards the characterization of biomaterial
2 489 systems. As shown in our experiments, highly folded conformations with very short end-to-
3 490 end distances may bring some difficulties for our simulator and lead to tricky simulations.
4 491 Indeed, in this case, the assembly of primitives would not respect the non-superposition
5 492 principle which is inherent to rigid bodies. Instead, we rather consider another major
6 493 conformational state arising from clustering to get a more stable mesoscopic simulation.
7

8 494 Finally, our objective is to perform simulations of more complex and larger fragments of
9 495 elastin, and even a full tropoelastin. These precious data would shed new light on the behavior
10 496 of elastin in the ageing process or as a biomaterial. Indeed, we would then be able to correlate
11 497 experimental data with parameters of our simulations, which would undoubtedly help us to
12 498 calibrate and improve our methodological approach. Furthermore, other ECM molecules
13 499 could be modeled by the CHLORAINE procedure and simulated in DURABIN, allowing us to get
14 500 a more realistic and comprehensive virtual model of the ECM.
15

16 501

17 502

18 503 **CRedit authorship contribution statement**

19 504 CD performed molecular dynamics and mesoscopic simulations, analyses, conception of the
20 505 library of patterns, wrote the paper, HW and JMC performed some molecular dynamics and
21 506 mesoscopic simulations, LD and SB offered their skills in the field of elastin peptides and
22 507 simulations, MD and NB wrote the paper and conceptualized the research, provided guidance
23 508 and supervision. All authors participated in the data interpretation and manuscript
24 509 preparation, reviewing and editing.
25

26 510

27 511 **Declaration of Competing Interest**

28 512 The authors declare that they have no known competing financial interests of personal
29 513 relationships that could have appeared to influence the work reported in this paper.
30

31 514

32 515 **Data availability**

33 516 Data will be available on request.
34

35 517

36 518

37
38
39
40
41
42
43
44
45
46
47
48
49
50
51
52
53
54
55
56
57
58
59
60
61
62
63
64
65

519 **Acknowledgments**

1
2 520 This work was supported by the project DURABIN (Region Champagne-Ardenne) and the chair
3
4 521 MAgICS (Grand Reims support). Part of this work was performed on computing resources
5
6 522 provided by CRIANN (Normandy, France) and Centre de Calcul Régional ROMEO (Université
7
8 523 de Reims Champagne Ardenne, France). It was granted by the Region Grand Est and the
9
10 524 Université de Reims Champagne Ardenne.

11 525

12
13 526

14
15 527

16
17 528

18
19 529

20
21 530

22
23 531

24
25 532

26
27 533

28
29 534

30
31 535

32
33 536

34
35 537

36
37 538

38
39 539

40
41 540

42
43 541

44
45 542

46
47 543

48
49 544

50
51 545

52
53 546

54
55 547

56
57 548

58
59 549

60 550

61

62

63

64

65

551 **References**

- 1
2 552 Baul, U., Bley, M., Dzubiella, J., 2020. Thermal Compaction of Disordered and Elastin-like
3 553 Polypeptides: A Temperature-Dependent, Sequence-Specific Coarse-Grained Simulation
4 554 Model. *Biomacromolecules* 21, 3523–3538. <https://doi.org/10.1021/acs.biomac.0c00546>
5 555 Brasseur, R., 1991. Differentiation of lipid-associating helices by use of three-dimensional
6 556 molecular hydrophobicity potential calculations. *J Biol Chem* 266, 16120–16127.
7 557 Cao, Q., Wang, Y., Bayley, H., 1997. Sequence of abductin, the molluscan ‘rubber’ protein.
8 558 *Current Biology* 7, R677–R678. [https://doi.org/10.1016/S0960-9822\(06\)00353-8](https://doi.org/10.1016/S0960-9822(06)00353-8)
9 559 Daura, X., Gademann, K., Jaun, B., Seebach, D., van Gunsteren, W.F., Mark, A.E., 1999.
10 560 Peptide Folding: When Simulation Meets Experiment. *Angewandte Chemie International*
11 561 *Edition* 38, 236–240.
12 562 Fauchère, J.-L., Quarendon, P., Kaetterer, L., 1988. Estimating and representing
13 563 hydrophobicity potential. *Journal of Molecular Graphics* 6, 203–206.
14 564 [https://doi.org/10.1016/S0263-7855\(98\)80004-0](https://doi.org/10.1016/S0263-7855(98)80004-0)
15 565 Furet, P., Sele, A., Cohen, N.C., 1988. 3D molecular lipophilicity potential profiles: a new
16 566 tool in molecular modeling. *Journal of Molecular Graphics* 6, 182–189.
17 567 [https://doi.org/10.1016/S0263-7855\(98\)80001-5](https://doi.org/10.1016/S0263-7855(98)80001-5)
18 568 Gosline, J., Lillie, M., Carrington, E., Guerette, P., Ortlepp, C., Savage, K., 2002. Elastic
19 569 proteins: biological roles and mechanical properties. *Phil. Trans. R. Soc. Lond. B* 357, 121–
20 570 132. <https://doi.org/10.1098/rstb.2001.1022>
21 571 Holst, M.J., Saied, F., 1995. Numerical solution of the nonlinear Poisson-Boltzmann
22 572 equation: Developing more robust and efficient methods. *J. Comput. Chem.* 16, 337–364.
23 573 <https://doi.org/10.1002/jcc.540160308>
24 574 Huang, J., Rauscher, S., Nawrocki, G., Ran, T., Feig, M., de Groot, B.L., Grubmüller, H.,
25 575 MacKerell, A.D., 2017. CHARMM36m: an improved force field for folded and intrinsically
26 576 disordered proteins. *Nat Methods* 14, 71–73. <https://doi.org/10.1038/nmeth.4067>
27 577 Humphrey, W., Dalke, A., Schulten, K., 1996. VMD: Visual molecular dynamics. *Journal of*
28 578 *Molecular Graphics* 14, 33–38. [https://doi.org/10.1016/0263-7855\(96\)00018-5](https://doi.org/10.1016/0263-7855(96)00018-5)
29 579 Ibáñez-Fonseca, A., Flora, T., Acosta, S., Rodríguez-Cabello, J.C., 2019. Trends in the design
30 580 and use of elastin-like recombinamers as biomaterials. *Matrix Biology* 84, 111–126.
31 581 <https://doi.org/10.1016/j.matbio.2019.07.003>
32 582 Jorda, J., Xue, B., Uversky, V.N., Kajava, A.V., 2010. Protein tandem repeats - the more
33 583 perfect, the less structured: Structural state of perfect protein repeats. *FEBS Journal* 277,
34 584 2673–2682. <https://doi.org/10.1111/j.1742-4658.2010.07684.x>
35 585 Le Page, A., Khalil, A., Vermette, P., Frost, E.H., Larbi, A., Witkowski, J.M., Fulop, T.,
36 586 2019. The role of elastin-derived peptides in human physiology and diseases. *Matrix Biology*
37 587 84, 81–96. <https://doi.org/10.1016/j.matbio.2019.07.004>
38 588 Li, N.K., Xie, Y., Yingling, Y.G., 2021. Insights into Structure and Aggregation Behavior of
39 589 Elastin-like Polypeptide Coacervates: All-Atom Molecular Dynamics Simulations. *J. Phys.*
40 590 *Chem. B* 125, 8627–8635. <https://doi.org/10.1021/acs.jpcc.1c02822>
41 591 Lins, L., Thomas, A., Brasseur, R., 2003. Analysis of accessible surface of residues in
42 592 proteins. *Protein Sci.* 12, 1406–1417. <https://doi.org/10.1110/ps.0304803>
43 593 Lyons, R.E., Lesieur, E., Kim, M., Wong, D.C.C., Huson, M.G., Nairn, K.M., Brownlee,
44 594 A.G., Pearson, R.D., Elvin, C.M., 2007. Design and facile production of recombinant resilin-
45 595 like polypeptides: gene construction and a rapid protein purification method. *Protein*
46 596 *Engineering, Design and Selection* 20, 25–32. <https://doi.org/10.1093/protein/gzl050>
47 597 MacEwan, S.R., Chilkoti, A., 2014. Applications of elastin-like polypeptides in drug delivery.
48 598 *Journal of Controlled Release* 190, 314–330. <https://doi.org/10.1016/j.jconrel.2014.06.028>
49 599 Muiznieks, L.D., Keeley, F.W., 2017. Biomechanical Design of Elastic Protein Biomaterials:
50 600 A Balance of Protein Structure and Conformational Disorder. *ACS Biomater. Sci. Eng.* 3,
51
52
53
54
55
56
57
58
59
60
61
62
63
64
65

601 661–679. <https://doi.org/10.1021/acsbiomaterials.6b00469>

1 602 Rodríguez-Cabello, J.C., Arias, F.J., Rodrigo, M.A., Girotti, A., 2016. Elastin-like
2 603 polypeptides in drug delivery. *Advanced Drug Delivery Reviews* 97, 85–100.
3 604 <https://doi.org/10.1016/j.addr.2015.12.007>

4 605 Rodríguez-Cabello, J.C., Gonzalez De Torre, I., González-Pérez, M., González-Pérez, F.,
5 606 Montequi, I., 2021. Fibrous Scaffolds From Elastin-Based Materials. *Front. Bioeng.*
6 607 *Biotechnol.* 9, 652384. <https://doi.org/10.3389/fbioe.2021.652384>

7 608 Seo, M., Rauscher, S., Pomès, R., Tieleman, D.P., 2012. Improving Internal Peptide
8 609 Dynamics in the Coarse-Grained MARTINI Model: Toward Large-Scale Simulations of
9 610 Amyloid- and Elastin-like Peptides. *J. Chem. Theory Comput.* 8, 1774–1785.
10 611 <https://doi.org/10.1021/ct200876v>

11 612 Tarakanova, A., Yeo, G.C., Baldock, C., Weiss, A.S., Buehler, M.J., 2018. Molecular model
12 613 of human tropoelastin and implications of associated mutations. *Proc Natl Acad Sci USA* 115,
13 614 7338–7343. <https://doi.org/10.1073/pnas.1801205115>

14 615 Tubiana, T., Carvaille, J.-C., Boulard, Y., Bressanelli, S., 2018. TTClust: A Versatile
15 616 Molecular Simulation Trajectory Clustering Program with Graphical Summaries. *J. Chem.*
16 617 *Inf. Model.* 58, 2178–2182. <https://doi.org/10.1021/acs.jcim.8b00512>

17 618 Wong, H., Crowet, J.-M., Dauchez, M., Ricard-Blum, S., Baud, S., Belloy, N., 2022.
18 619 Multiscale modelling of the extracellular matrix. *Matrix Biology Plus* 13, 100096.
19 620 <https://doi.org/10.1016/j.mbplus.2021.100096>

20 621 Wong, H., PrévotEAU-Jonquet, J., Baud, S., Dauchez, M., Belloy, N., 2018. Mesoscopic Rigid
21 622 Body Modelling of the Extracellular Matrix Self-Assembly. *Journal of Integrative*
22 623 *Bioinformatics* 15. <https://doi.org/10.1515/jib-2018-0009>

23 624 Zhou, C.-Z., 2000. Fine organization of Bombyx mori fibroin heavy chain gene. *Nucleic*
24 625 *Acids Research* 28, 2413–2419. <https://doi.org/10.1093/nar/28.12.2413>

25 626

26 627

27 628

28 629

29 630

30 631

31 632

32 633

33 634

34 635

35 636

36 637

37 638

38 639

39 640

40 641

41

42

43

44

45

46

47

48

49

50

51

52

53

54

55

56

57

58

59

60

61

62

63

64

65

642 **Figure captions**

1
2 643

3
4 644 Figure 1: Representation and size of a collagen type IV (A), of a monomer of tropoelastin (B),
5
6 645 of the assembly of 4 monomers of tropoelastin (C) and of a [VGLAPG(VGVAPG)₂]₂₇ r-ELP (D).

7
8 646 **Scale refers to the four structures.**

9
10 647 **Figure 2: Molecular surface of one representative conformation for the 4 main clusters of r-**
11
12 648 **ELP [VGLAPG(VGVAPG)₂] represented with Blender and used as primitives. The probability of**
13
14 649 **occurrence of each conformation is provided.**

15 650 Figure 3: Definition of colliders and joints for an elastic pattern.

16
17 651 Figure 4: View of the 4 r-ELP systems modeled in the mesoscope in an extended form at the
18
19 652 beginning of each simulation.

20
21 653 Figure 5: Evolution of 10 chains of [(VGLAPG)(VGVAPG)₂]₂₇ during the first 6,000 steps of a
22
23 654 CHLORAINE procedure using both electrostatic and MHP potentials.

24
25 655 Figure 6: Matrices of interactions of the polypeptide (VPGEG)₂₇ after 38,000 steps (A) and
26
27 656 128,000 steps (B).

28
29 657 Figure 7: (VPGVG)₂₇ interactions without contribution (A), with electrostatics (B), with MHP
30
31 658 (C) and with both electrostatics and MHP (D).

32
33 659 Table 1: Number of steps reached by the simulation (60 h) for the 4 systems in 4 different
34
35 660 conditions: neutral (no added contribution), MHP (hydrophobicity/hydrophilicity
36
37 661 contribution), electrostatics (electrostatic contribution) and both (MHP + electrostatic)
38
39 662 contributions.

40
41 663 Table 2: Mean number of intermolecular contacts per simulation step, for the 4 systems in the
42
43 664 4 conditions (same conditions as the previous Table 1).

44 665

45
46 666

47
48 667

49
50 668

51
52 669

53
54 670

55
56 671

57
58 672

59
60 673

61

62

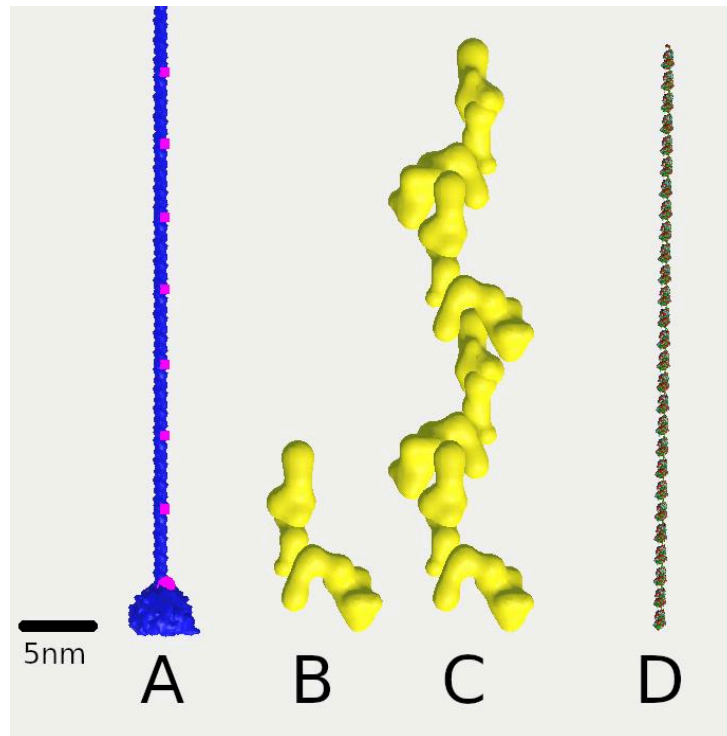
63

64

65

674 **List of Figures**

675



676

677 Figure 1: Representation and size of a collagen type IV (A), of a monomer of tropoelastin (B),
678 of the assembly of 4 monomers of tropoelastin (C) and of a $[VGLAPG(VGVAPG)_2]_{27}$ r-ELP (D).

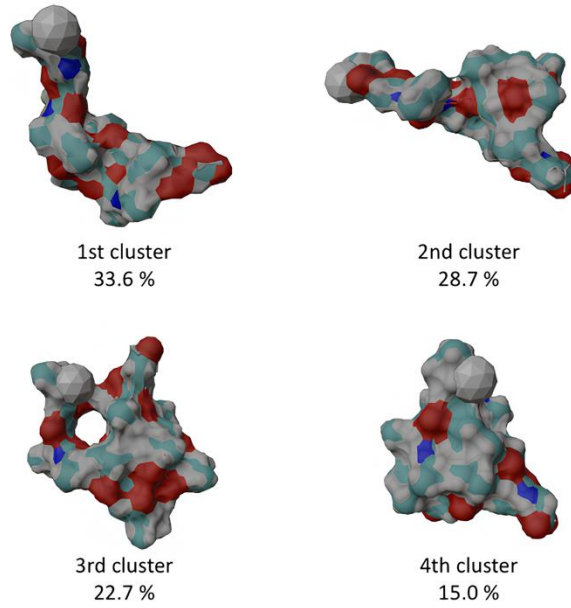
679

Scale refers to the four structures.

680

681

1
2
3
4
5
6
7
8
9
10
11
12
13
14
15
16
17
18
19
20
21
22
23
24
25
26
27
28
29
30
31
32
33
34
35
36
37
38
39
40
41
42
43
44
45
46
47
48
49
50
51
52
53
54
55
56
57
58
59
60
61
62
63
64
65



682

683

Figure 2: Molecular surface of one representative conformation for the 4 main clusters of r-

684

ELP [VGLAPG(VGVAPG)₂] represented with Blender and used as primitives. The probability of

685

occurrence of each conformation is provided.

686

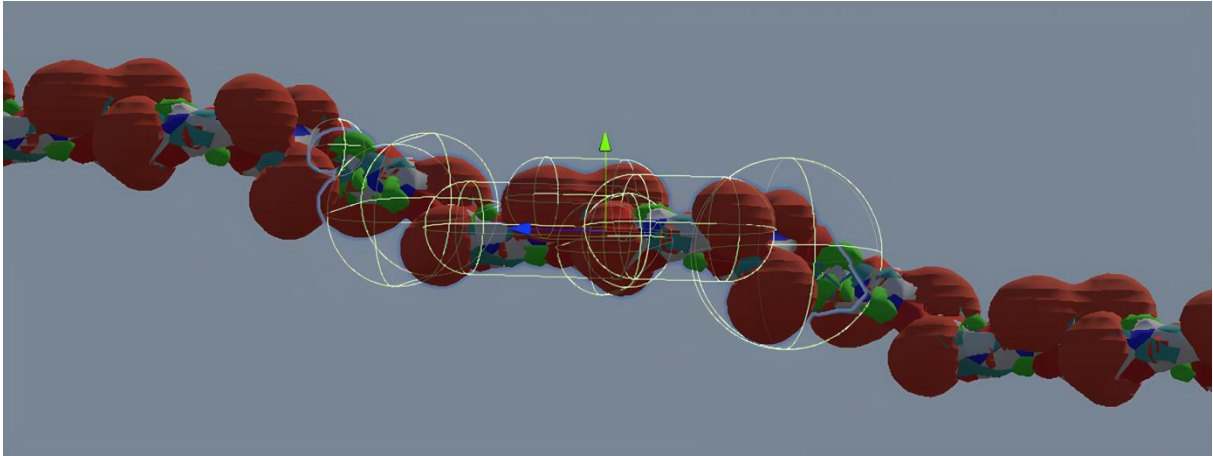


Figure 3: Definition of colliders and joints for an elastic pattern.

1
2
3
4
5
6
7
8
9
10
11
12
13
14
15
16
17
18
19
20
21
22
23
24
25
26
27
28
29
30
31
32
33
34
35
36
37
38
39
40
41
42
43
44
45
46
47
48
49
50
51
52
53
54
55
56
57
58
59
60
61
62
63
64
65

687

688

689

690

1
2
3
4
5
6
7
8
9
10
11
12
13
14
15
16
17
18
19
20
21
22
23
24
25
26
27
28
29
30
31
32
33
34
35
36
37
38
39
40
41
42
43
44
45
46
47
48
49
50
51
52
53
54
55
56
57
58
59
60
61
62
63
64
65

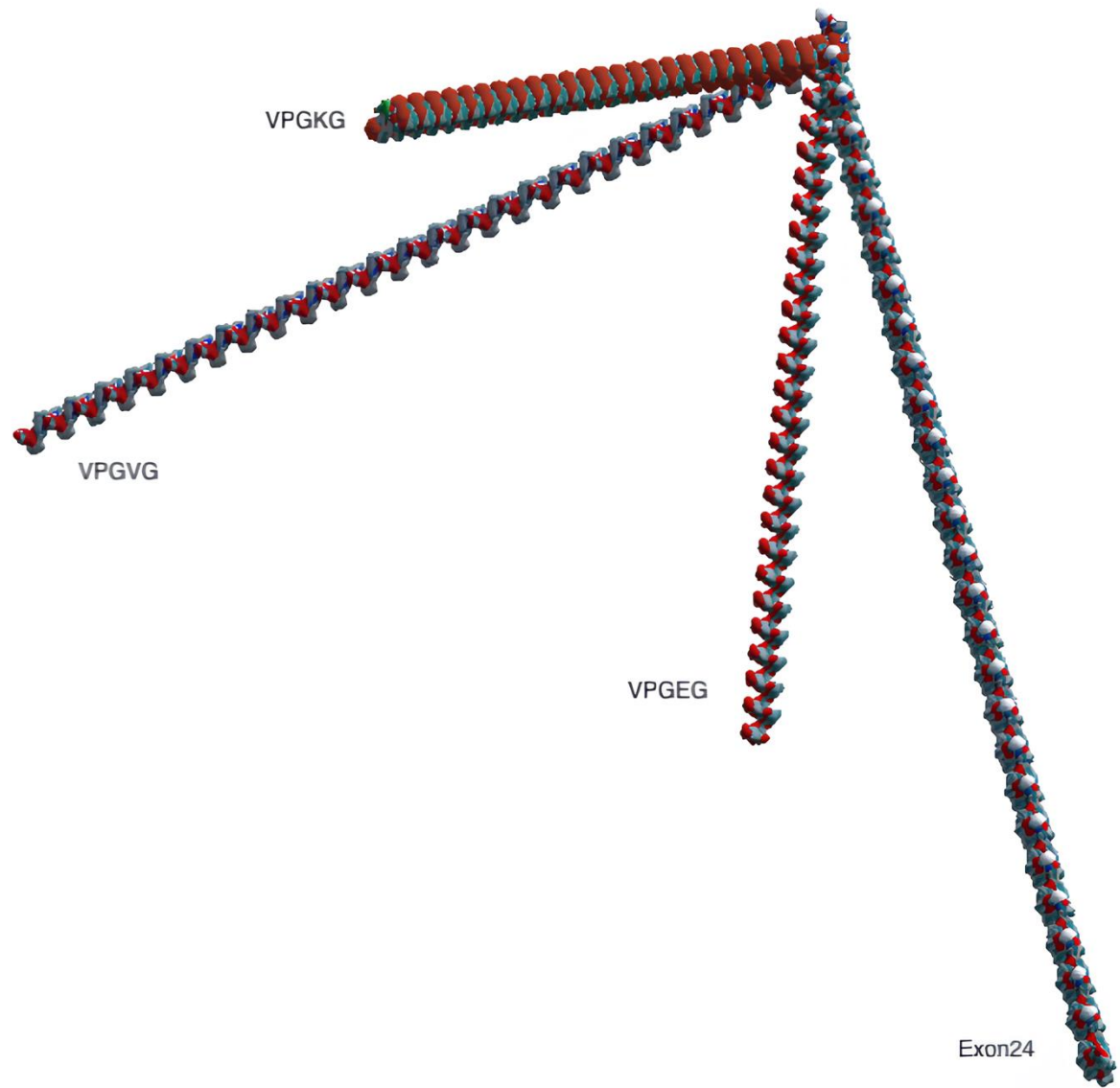
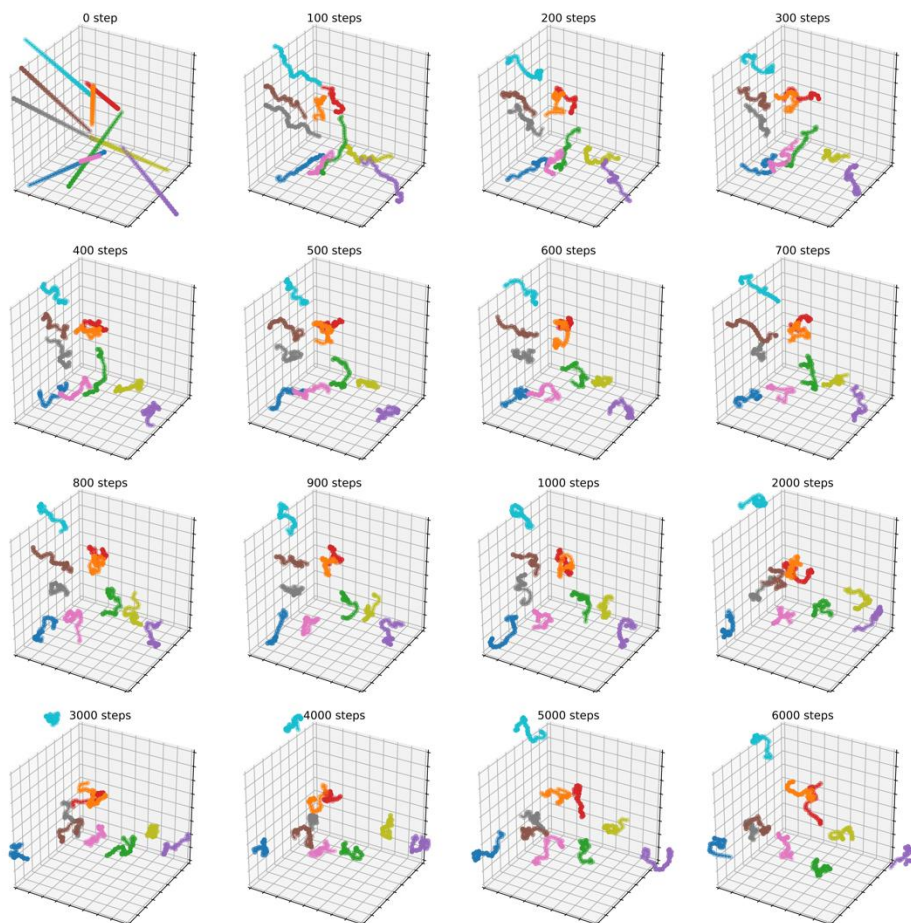


Figure 4: View of the 4 r-ELP systems modeled in the mesoscope in an extended form at the beginning of each simulation.



31 695

32 696

Figure 5: Evolution of 10 chains of $[(VGLAPG)(VGVAPG)_2]_{27}$ during the first 6,000 steps of a CHLORAINE procedure using both electrostatic and MHP potentials.

35 697

37 698

1
2
3
4
5
6
7
8
9
10
11
12
13
14
15
16
17
18
19
20
21
22
23
24
25
26
27
28
29
30
38
39
40
41
42
43
44
45
46
47
48
49
50
51
52
53
54
55
56
57
58
59
60
61
62
63
64
65

1
2
3
4
5
6
7
8
9
10
11
12
13
14
15
16
17 699
18 700
19 701
20 702
21 703
22
23
24
25
26
27
28
29
30
31
32
33
34
35
36
37
38
39
40
41
42
43
44
45
46
47
48
49
50
51
52
53
54
55
56
57
58
59
60
61
62
63
64
65

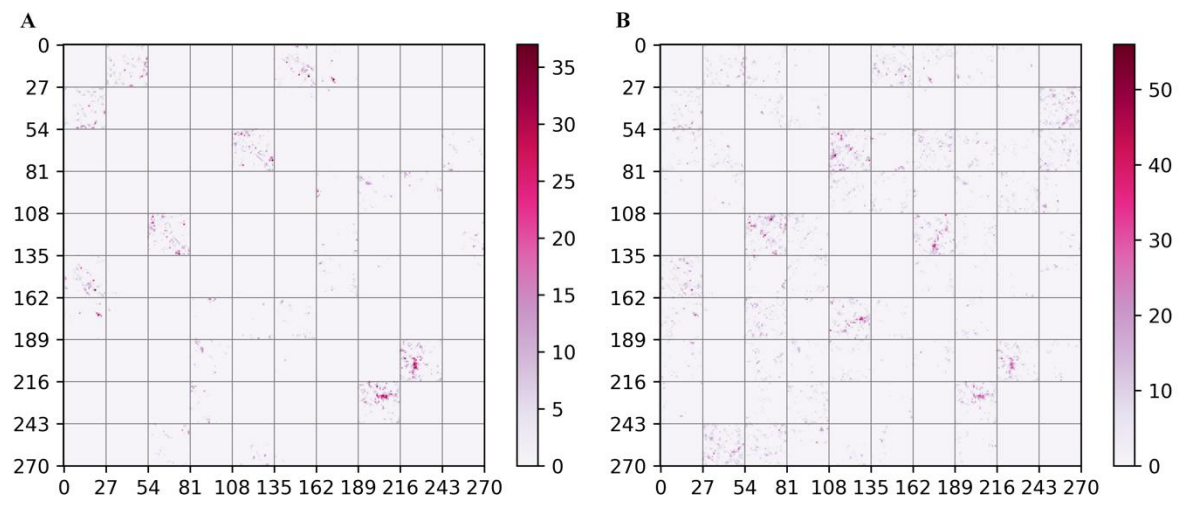


Figure 6: Matrices of interactions of the polypeptide (VPGEG)₂₇ after 38,000 steps (A) and 128,000 steps (B).

1
2
3
4
5
6
7
8
9
10
11
12
13
14
15
16
17
18
19
20
21
22
23
24
25
26
27
28
29
30
31
32
33
34
35
36
37
38
39
40
41
42
43
44
45
46
47
48
49
50
51
52
53
54
55
56
57
58
59
60
61
62
63
64
65

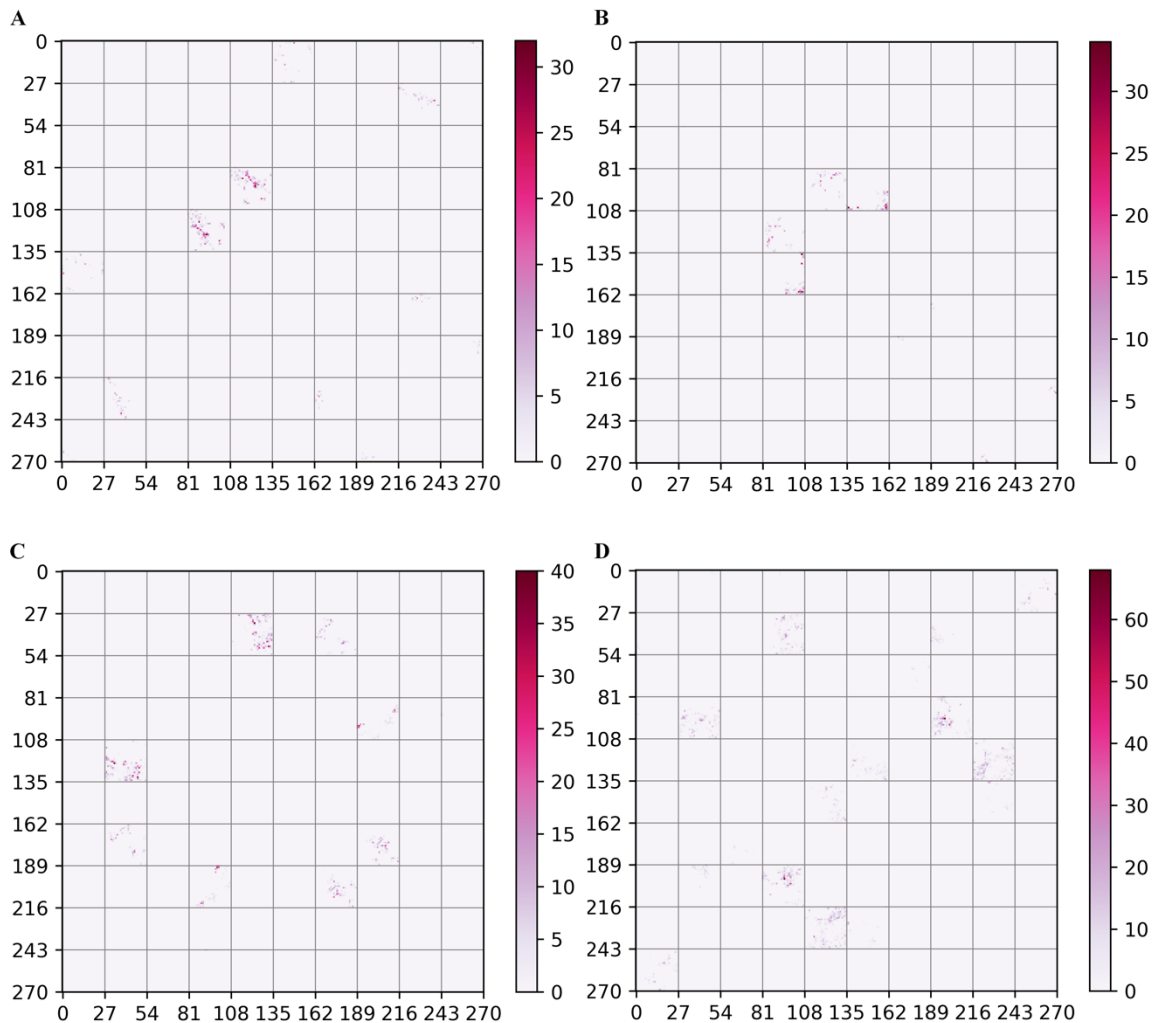


Figure 7: (VPGVG)₂₇ interactions without contribution (A),
with electrostatics (B), with MHP (C) and with both electrostatics and MHP (D).

709 **List of Tables**

1
2
3
4
5
6
7
8
9
10
11
12
13
14
15
16
17
18
19
20
21
22
23
24
25
26
27
28
29
30
31
32
33
34
35
36
37
38
39
40
41
42
43
44
45
46
47
48
49
50
51
52
53
54
55
56
57
58
59
60
61
62
63
64
65

710

711
712
713
714
715
716
717
718

	Neutral	MHP	Electrostatics	Both
VPGVG	46,680	4,610	30,460	4,330
VPGEG	128,110	25,550	52,490	11,570
VPGKG	38,220	8,650	31,330	11,230
« Exon24 »	46,260	4,810	33,010	4,410

Table 1: Number of steps reached by the simulation (60 h) for the 4 systems in 4 different conditions: neutral (no added contribution), MHP (hydrophobicity/hydrophilicity contribution), electrostatics (electrostatic contribution) and both (MHP + electrostatic contributions).

		Neutral	MHP	Electrostatics	Both
	VPGVG	0.63	1.03	0.38	2.36
	VPGEG	0.44	0.74	0.32	0.99
	VPGKG	2.38	0.25	1.40	2.80
	« Exon24 »	0.52	1.89	0.34	0.17

719

720

Table 2: Mean number of intermolecular contacts per simulation step, for the 4 systems in the 4 conditions (same conditions as the previous Table 1).

721

722

1
2
3
4
5
6
7
8
9
10
11
12
13
14
15
16
17
18
19
20
21
22
23
24
25
26
27
28
29
30
31
32
33
34
35
36
37
38
39
40
41
42
43
44
45
46
47
48
49
50
51
52
53
54
55
56
57
58
59
60
61
62
63
64
65

CRediT authorship contribution statement

CD performed molecular dynamics and mesoscopic simulations, analyses, conception of the library of patterns, wrote the paper, HW and JMC performed some molecular dynamics and mesoscopic simulations, LD and SB offered their skills in the field of elastin peptides and simulations, MD and NB wrote the paper and conceptualized the research, provided guidance and supervision. All authors participated in the data interpretation and manuscript preparation, reviewing and editing.